# Molecular and Multimodality Imaging in Cardiovascular Disease

Thomas H. Schindler
Richard T. George
Joao A.C. Lima
*Editors*

Springer

# Molecular and Multimodality Imaging in Cardiovascular Disease

Thomas H. Schindler • Richard T. George
Joao A.C. Lima
Editors

# Molecular and Multimodality Imaging in Cardiovascular Disease

Springer

*Editors*
Thomas H. Schindler
Johns Hopkins University
Radiology School of Medicine
Cardiovascular Nuclear Medicine
Baltimore, MD
USA

Joao A.C. Lima
Radiology and Epidemiology
Johns Hopkins University
School of Medicine, Cardiology
Baltimore, MD
USA

Richard T. George
Johns Hopkins University
School of Medicine, Cardiology
Baltimore, MD
USA

ISBN 978-3-319-19610-7 ISBN 978-3-319-19611-4 (eBook)
DOI 10.1007/978-3-319-19611-4

Library of Congress Control Number: 2015945382

Springer Cham Heidelberg New York Dordrecht London


Printed on acid-free paper

Springer International Publishing AG Switzerland is part of Springer Science+Business Media (www.springer.com)

# Preface

Within the last decade of technical advancements, the field in cardiovascular imaging has rapidly expanded to a variety of modalities to image morphology and function with cardiac PET/MRI, CT, PET/CT, and SPECT/CT. These advanced imaging techniques now provide noninvasive coronary angiograms, unique and detailed information into the coronary arterial wall, description of cardiac structure and function, and complementary functional information as regards myocardial blood flow and perfusion, viability, and "vulnerable" arterial plaque burden. These cardiovascular imaging modalities may alter current paradigms for diagnosis and cardiovascular risk stratification while raising new questions and discussions for the researcher and clinician in this field. In view of this rapid evolution of molecular and multimodality imaging, the editors have strived to provide a comprehensive textbook that captures the full scope, potential, and promise of cardiac PET/MRI, CT, PET/CT, and SPECT/CT in imaging cardiovascular disease.

The editors have succeeded to recruit internationally renowned panel of expert authors, who are leading authorities in their respective disciplines. This book edition of *Molecular and Multimodality Imaging in Cardiovascular Disease* provides in-depth, comprehensive discussion of technical characteristics and clinical applications of each advanced imaging modality, implying their comparative strengths and weaknesses.

The first three chapters focus on physics; instrumentation, and systems of the PET/MRI; potential cardiac application; and initial experience. This is followed by chapters describing the evolving role of PET/CT in the detection and characterization of cardiac sarcoid disease and different imaging modalities to signify cardiac amyloidosis. There is also an in-depth discussion of the clinical significance in identifying hibernating-stunning myocardium in ischemic cardiomyopathy with different imaging modalities such as PET/CT, SPECT/CT, MRI, and echocardiography and how these imaging modalities may complement each other for a further refinement of viability assessment. Principles of cardiac MRI in conjunction with T1 mapping to determine extracellular volume fraction as surrogate marker of interstitial fibrosis and potential clinical value are excellently addressed. The second part of chapters focus on the exciting role of multimodality imaging in the detection of the "vulnerable" arterial plaque, the concurrent assessment of coronary morphology and myocardial perfusion or myocardial blood flow with a fused three-dimensional

display, and, finally, the added prognostic value of coronary artery calcification measurements to myocardial perfusion imaging.

Noninvasive imaging modalities have become important tools for all physicians involved in the diagnosis and treatment of cardiovascular disease. PET/MRI, CT, PET/CT, and SPECT/CT confer a great potential to shed more light on cardiovascular pathophysiology, providing a framework for early diagnosis and treatment effectiveness of novel therapeutic treatment options. The current book edition is anticipated to contribute importantly to an understanding of the potential of noninvasive, molecular, and multimodality imaging in cardiovascular disease.

Baltimore, MD, USA Thomas H. Schindler, MD

# Contents

# Contributors

**Mouaz H. Al-Mallah, MD, MSc, FACC, FAHA, FESC** Cardiac Imaging, King Abdul-Aziz Cardiac Center, King Abdul-Aziz Medical City (Riyadh), National Guard Health Affairs, Riyadh, Kingdom of Saudi Arabia

**Brian Mc Ardle, MD** Division of Cardiology, University of Ottawa Heart Institute, Canadian Molecular Imaging Center of Excellence (CMICE), Ottawa, ON, Canada

**Sharmila Dorbala, MD, MPH, FACC** Noninvasive Cardiovascular Imaging Program, Departments of Radiology and Medicine (Cardiology), Heart and Vascular Center, Boston, MA, USA

Cardiac Amyloidosis Program, Department of Medicine, Boston, MA, USA

Brigham and Women's Hospital, Harvard Medical School, Boston, MA, USA

**Marc R. Dweck, MD, PhD** Centre for Cardiovascular Science, University of Edinburgh, Edinburgh, UK

Clinical Research Imaging Centre, University of Edinburgh, Edinburgh, UK

Heart Centre, Edinburgh, UK

**Oliver Gaemperli, MD** Department of Nuclear Medicine, University Hospital Zurich, Zurich, Switzerland

University Heart Center, Zuerich, Switzerland

**Richard T. George, MD** Johns Hopkins University, School of Medicine, Cardiology, Baltimore, MD, USA

**Nikhil V. Joshi, MD** Centre for Cardiovascular Science, University of Edinburgh, Edinburgh, UK

Clinical Research Imaging Centre, University of Edinburgh, Edinburgh, UK

Heart Centre, Edinburgh, UK

**Philipp A. Kaufmann, MD** Department of Nuclear Medicine, University Hospital Zurich, Zurich, Switzerland

University Heart Center, Zuerich, Switzerland

**Paul Knaapen, MD** Department of Cardiology, VU University Medical Center of Amsterdam, Amsterdam, The Netherlands

**Karl P. Kunze, MSc** Nuklearmedizinische Klinik und Poliklinik, Klinikum rechts der Isar, Technische Universität München, Munich, Germany

**Eugene Leung, MD, FRCPC** Division of Cardiology, University of Ottawa Heart Institute, Canadian Molecular Imaging Center of Excellence (CMICE), Ottawa, ON, Canada

**Joao A.C. Lima, MD** Radiology and Epidemiology, Johns Hopkins University, School of Medicine, Cardiology, Baltimore, MD, USA

**Stephan G. Nekolla, PhD** Nuklearmedizinische Klinik und Poliklinik, Klinikum rechts der Isar, Technische Universität München, Munich, Germany

**Felix Nensa, MD** Department of Diagnostic and Interventional Radiology, University Hospital of Essen, University of Duisburg-Essen, Essen, Germany

**David E. Newby, MD, PhD** Centre for Cardiovascular Science, University of Edinburgh, Edinburgh, UK

Clinical Research Imaging Centre, University of Edinburgh, Edinburgh, UK

Heart Centre, Edinburgh, UK

**Hiroshi Ohira, MD** Division of Cardiology, University of Ottawa Heart Institute, Canadian Molecular Imaging Center of Excellence (CMICE), Ottawa, ON, Canada

**Aju P. Pazhenkottil, MD** Department of Nuclear Medicine, University Hospital Zurich, Zurich, Switzerland

University Heart Center, Zurich, Switzerland

**Matthieu Pelletier-Galarneau, MD, MSc** Division of Cardiology, University of Ottawa Heart Institute, Canadian Molecular Imaging Center of Excellence (CMICE), Ottawa, ON, Canada

**Thorsten D. Poeppel, MD** Department of Diagnostic and Interventional Radiology, University Hospital of Essen, University of Duisburg-Essen, Essen, Germany

**Harald H. Quick, PhD** Department of Diagnostic and Interventional Radiology, High Field and Hybrid MR Imaging, University Hospital Essen, Essen, Germany

Erwin L. Hahn Institute for MR Imaging, University of Duisburg-Essen, Essen, Germany

**Christoph Rischpler, MD** Nuklearmedizinische Klinik und Poliklinik, Klinikum rechts der Isar, Technische Universität München, Munich, Germany

**Terrence D. Ruddy, MD, FRCPC, FACC** Division of Cardiology, University of Ottawa Heart Institute, Canadian Molecular Imaging Center of Excellence (CMICE), Ottawa, ON, Canada

**Erik B. Schelbert, MD, MS** Division of Cardiology, Department of Medicine, University of Pittsburgh, Pittsburg, PA, USA

**Thomas H. Schindler, MD** Johns Hopkins University, Radiology School of Medicine, Cardiovascular Nuclear Medicine, Baltimore, MD, USA

**Thomas Schlosser, MD** Department of Diagnostic and Interventional Radiology, University Hospital of Essen, University of Duisburg-Essen, Essen, Germany

**Ravi K. Sharma, MD** Division of Cardiology, Department of Medicine, Johns Hopkins University, Baltimore, MA, USA

**Ines Valenta, MD** Department of Radiology SOM, Nuclear Medicine, Johns Hopkins University, Baltimore, MA, USA

**Timothy C. Wong, MD, MS** Division of Cardiology, Department of Medicine, University of Pittsburgh, Pittsburg, PA, USA

**Xiaoli Zhang, MD, PhD** Department of Nuclear Medicine, State Key Laboratory of Cardiovascular Disease, Fuwai Hospital, National Center for Cardiovascular Diseases, Chinese Academy of Medical Sciences and Peking Union Medical College, Beijing, People's Republic of China

# PET/MRI: Physics, Instrumentation, and Systems

1

Harald H. Quick

## 1.1 Introduction

Hybrid imaging with combined positron emission tomography/magnetic resonance imaging (PET/MRI) is the most recent addition to the palette of hybrid imaging modalities [1, 2]. PET/MRI synergistically combines the excellent soft tissue contrast and detailed image resolution of MR imaging with metabolic information provided by PET. Integrated PET/MRI systems furthermore offer the ability to acquire hybrid imaging data simultaneously [1, 3]. Beyond exact co-registration of PET and MR imaging data, this can be applied for MR-based motion correction of PET data. Especially in the context of diagnostic cardiac imaging, these features open up several applications, e.g., evaluation of cardiac function and viability and diagnosis of cardiac inflammatory diseases and tumorous diseases [4–7]. To fully assess the diagnostic potential of PET/MR, however, several physical and technical challenges had to be overcome and are still subject to ongoing research. Due to the absence of CT information, attenuation correction (AC) of the patient tissues in PET/MRI has to be based on MR images which are currently limited in the number of tissue classes available [8] and by undercorrection of the bone tissue [9]. Dedicated cardiac radiofrequency (RF) coils, necessary for reception of the MR signal, and ECG gating equipment are currently not considered in AC. Consequently quantification of cardiac PET data in PET/MRI, therefore, might be biased. Furthermore, the clinical workflow is rather complex and needs to be tailored to cardiac examinations.

H.H. Quick, PhD
Erwin L. Hahn Institute for MR Imaging, University of Duisburg-Essen, Essen, Germany

Department of High Field and Hybrid MR Imaging,
University Hospital Essen, Essen, Germany
e-mail: harald.quick@uni-due.de



T.H. Schindler et al. (eds.), *Molecular and Multimodality Imaging in Cardiovascular Disease*, DOI 10.1007/978-3-319-19611-4_1

In this chapter, current PET/MRI system designs are presented, physical challenges and methodological solutions for attenuation and motion correction are discussed, and furthermore, specific challenges of cardiac PET/MR hybrid imaging will be highlighted.

## 1.2 PET/MRI System Design

The combination of separate PET and MRI systems into a single multimodality system needed a careful design of several hardware components [1, 3]. MR imaging requires well-controlled and uniform static magnetic fields for spin polarization, linear gradient fields for spatial signal encoding, and radiofrequency fields for spin excitation and signal readout. Therefore, any unshielded additional electronic hardware can affect the accuracy and quality of MR images. On the other hand, conventional PET detectors and associated hardware and electronics are not designed for the use inside strong electromagnetic fields. In particular, PET detectors based on photomultiplier tubes (PMTs), which are needed to convert and amplify signal from scintillation crystals into electronic signal, do not function properly in or near strong magnetic fields [10, 11].

Integrating PET detectors based on PMT within an MR system has proven to be a difficult task, requiring vendors to either opt for avalanche photodiodes (APDs) [10, 11] or physically separate the PET and MR imaging units [2]. The performance of APD detectors, used to replace PMT, is not affected by strong magnetic fields [10, 11]. In the context of PET/MR hybrid imaging, conventional PMT detectors can only be used if the PET unit is placed sufficiently far away from the MR imaging unit such that the magnetic field strength at the position of the PET unit is very low [2]. A recently available integrated PET/MRI system contains new semiconductor detectors, e.g., silicon photon multipliers (SiPMs) [12, 13]. Like APD detectors, SiPM detectors are not sensitive to the magnetic field and, consequently, can be integrated inside an MR system. Four current PET/MR hybrid imaging systems are shown in Fig. 1.1. A schematic drawing of an integrated PET/MRI system and MR-compatible APD-based PET detectors are displayed in Fig. 1.2.

## 1.3 Attenuation Correction

### 1.3.1 Attenuation Correction in PET/CT

A technical challenge in PET/MR hybrid imaging is the attenuation correction of PET emission images based on MR information, necessary for an accurate quantitative measurement of the tracer activity concentration. In PET/CT hybrid imaging, the CT image providing spatial representation of Hounsfield units (HU) of the patient tissues and hardware components, such as patient table, can be used to calculate attenuation maps (μ-maps) by applying an appropriate energy scaling (Fig. 1.3). This is achieved by using the inherent 3D CT data of the patient tissues and patient table. The CT data (in HU) is then directly

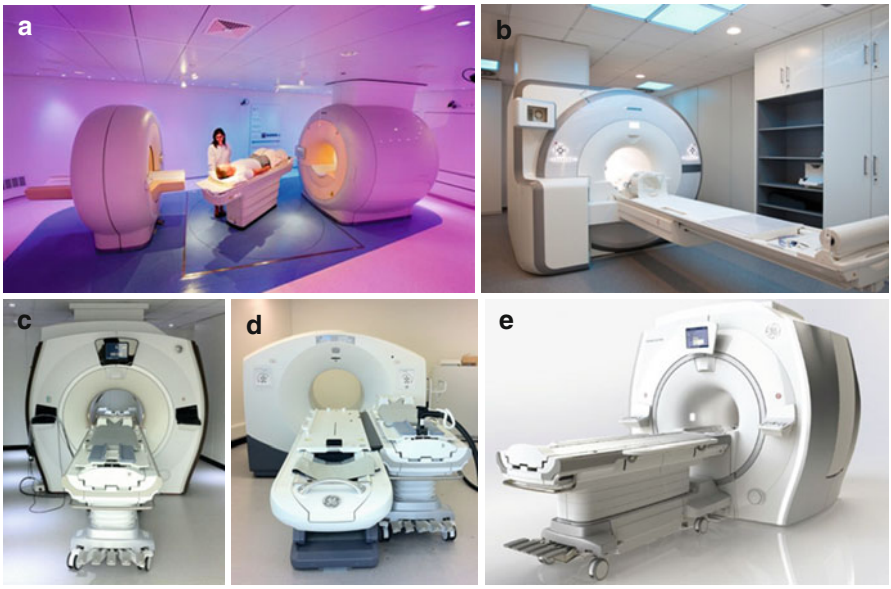


**Fig. 1.1** Four current systems for PET/MR hybrid imaging: (**a**) Philips Ingenuity TF, (**b**) Siemens Biograph mMR, (**c**, **d**) GE Tri-modality MR (**c**) and PET/CT (**d**) connected via a patient table shuttle system, (**e**) GE Signa PET/MR. All four systems perform at 3 Tesla field strength. Systems (**a**) and (**c**, **d**) provide sequential PET/MR examinations while systems (**b**) and (**e**) allow for simultaneous PET and MR data acquisition

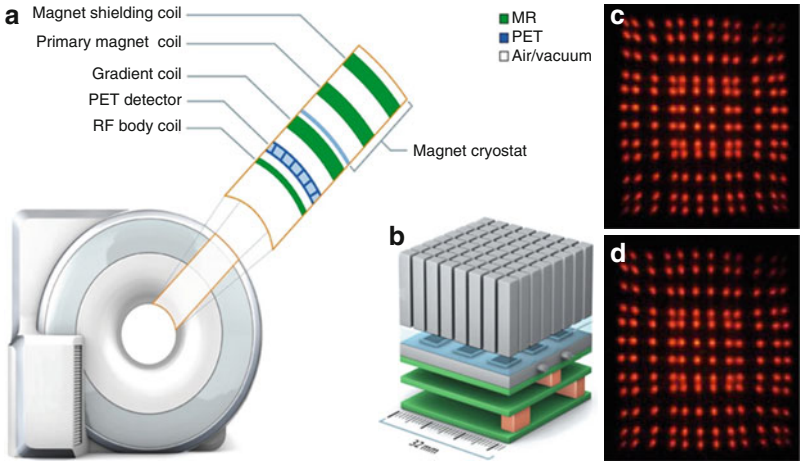


**Fig. 1.2** (**a**) Schematic drawing of an integrated PET/MR system (Biograph mMR, Siemens AG, Healthcare Sector). The drawing shows the integration of the PET detectors in the MR system structure. From the inside to the outside: radiofrequency body coil, PET detector, gradient coil assembly, primary magnet coil, and magnet shielding coil. (**b**) PET detector block assembly where 64 lutetium oxyorthosilicate (LSO) crystals form one detector block that are read out by MR-compatible avalanche photodiode (APD) detectors. (**c**, **d**) Demonstration of the MR compatibility of an LSO crystal with APD-based PET detector. The PET signal footprint in (**c**) was acquired without magnetic field, while the signal footprint in (**d**) was acquired at 7.0 Tesla magnetic field strength. No magnetic field-related signal distortions can be seen in (**d**) (**c**, **d** from Lecomte et al. [11])

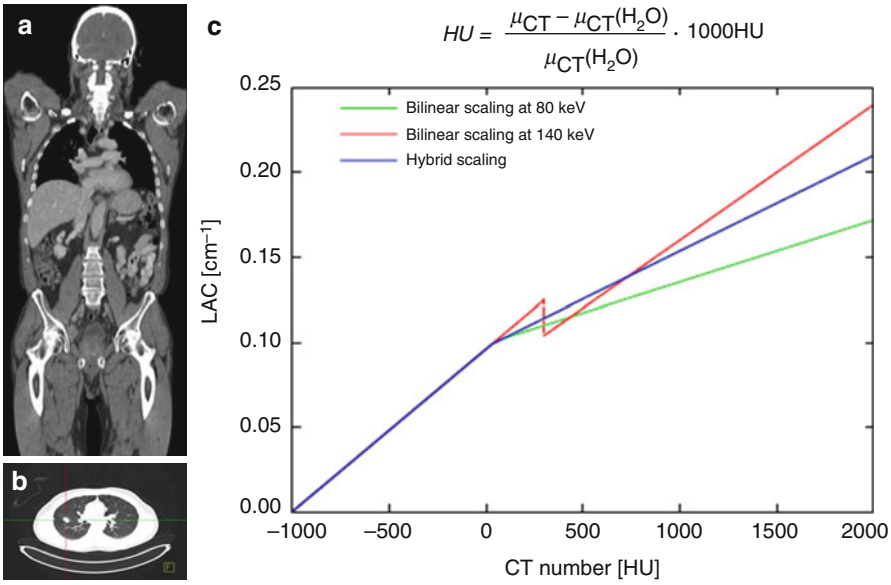


**Fig. 1.3** Attenuation correction of PET data in PET/CT hybrid imaging. In PET/CT, attenuation correction is achieved by synergistically using the inherent three-dimensional CT data of the patient tissues (**a**) and patient table (**b**). The CT data (Hounsfield Units, HU) is then directly converted from its energy level (e.g., 80–140 keV) by bilinear conversion models (From Carney et al. [14]) to linear attenuation coefficients (LAC) of PET at 511 keV energy level (**c**)

converted from its energy level (e.g., 80–140 keV) by bilinear conversion models to linear attenuation coefficients (LAC) of PET at 511 keV energy level (Fig. 1.3) [14].

### 1.3.2 Attenuation Correction in PET/MRI

PET data needs to be attenuation corrected in the reconstruction process in order to provide a valid quantification of tracer activity distribution in the human body. Scanner hardware components (e.g., tabletop, RF coils) as well as patient tissues within the FOV of the PET detector during data acquisition attenuate the number of true annihilation events and consequently may lead to false results without providing AC. Depending on the position of the heart in the thorax, photons emitted from the myocardium may experience different attenuations on their way through different body tissues to the PET detector. Non-AC PET data generally shows underestimation of the real tracer activity deep in the patient's body and also in the heart. Since the PET/MRI system cannot measure linear attenuation directly as in PET/CT hybrid imaging, AC here needs to be performed differently (Fig. 1.4).

#### 1.3.2.1 Attenuation Correction of Patient Tissues

Attenuation correction of human soft tissue is necessary to correct for the individual patient anatomy. Since no linear attenuation coefficient-based CT information is

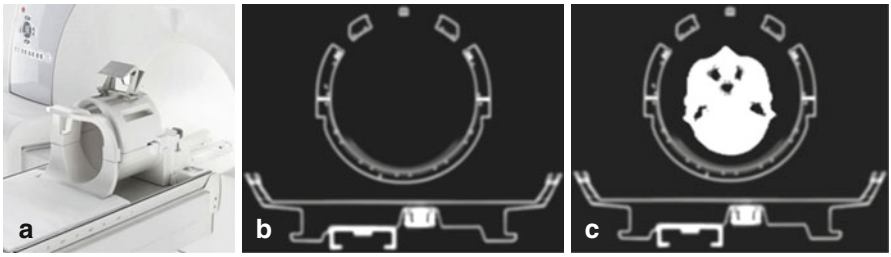


**Fig. 1.4** Attenuation correction PET/MR hybrid imaging. Photograph (**a**) shows a head/neck radiofrequency coil that was optimized for PET transparency for use in an integrated PET/MR hybrid system. Image (**b**) shows a transversal view through the CT-based hardware attenuation map of a PET/MR system's patient table with a radiofrequency head coil in place. In image (**c**) the MR-based attenuation correction map of the patient tissues (head) has been added. Thus (**c**) shows the completed attenuation map that represents the geometric distribution of attenuating hardware and soft tissue structures in the PET field of view

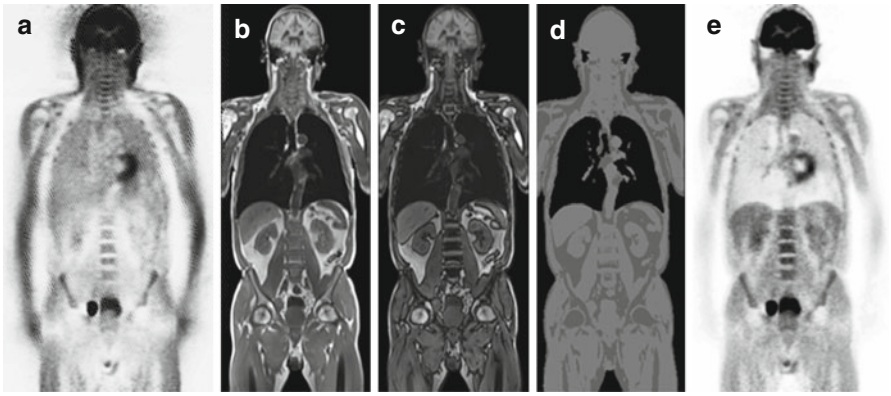


**Fig. 1.5** Patient-tissue attenuation correction based on MR imaging. (**a**) Uncorrected whole-body PET scan showing relative activity enhancement in the lungs and along the outer contours of the patient. (**b**, **c**) Dixon-based MR sequence providing separate water/fat "in-phase" and "opposed-phase" images that serve as basis for soft tissue segmentation. (**d**) Segmented soft tissue groups (air, fat, muscle, lungs) that can be assigned to a PET attenuation map of the patient tissues. (**e**) Resulting attenuation-corrected PET scan of the initial data set (**a**). *Note*: Bone signal is assigned as soft tissue values in this MR-based approach for AC

available in integrated PET/MRI, tissue-specific AC has to be based on MR information which is based on proton density and relaxation properties (e.g., T1 and T2 relaxation times), rather than on the attenuation of X-rays in tissue. Both air and solid bones lack signal in MRI; thus these fundamentally different tissue classes are difficult to separate. In the current implementation of integrated PET/MRI systems, tissue attenuation and scatter correction is performed using a three-dimensional (3D) Dixon-based MR imaging technique, providing two sets of images where water and fat are "in phase" and "out of phase" (Fig. 1.5) [8]. This allows reconstruction of fat-only, water-only, and fat-water images and results in tissue segmentation of air, fat, muscle, and lungs in the reconstructed and displayed μ-maps

(Fig. 1.5) [8]. The cortical bone is currently not being accounted for in the Dixon-based AC approach. The bone is here classified as soft tissue, and thus the exact magnitude of PET signal attenuation of the bone might be underestimated [9].

#### 1.3.2.2 Attenuation Correction of System Hardware Components

Radiofrequency surface receiver coils are a technical precondition for high-resolution MR imaging and are well established in clinical MRI. In a standard setup of integrated PET/MR cardiac imaging, the patient is placed on top of a rigid phased-array spine RF coil. For anterior signal detection, a second multichannel phased-array RF surface coil is placed on the thorax of the patient during simultaneous MR and PET data acquisition (Fig. 1.6). Thus, all RF surface coils used in the PET field of view during simultaneous PET data acquisition have to be optimized for PET transparency, i.e., such coils should attenuate the photons only minimally [15–18].

The PET signal attenuation of rigid and stationary equipment such as the RF spine array and the RF head/neck coil can be compensated for by straightforward AC methods. After scanning this equipment by using CT, a 3D map of attenuation values can be generated. This data can then be converted into a 3D representation of the 511 keV attenuation values, the so-called μ-map. By linking the RF spine or RF head coil's position to the patient's table position, the corresponding AC μ-map for each table position is automatically selected by the system for PET image reconstruction [17].

For flexible surface RF coils like the 6-channel RF body phased array (Fig. 1.6) which may be used in the context of cardiac PET/MR, the AC is performed differently. Because the design of such surface RF coils is flexible, the individual position and shape of this RF coil during a patient examination is not known. Thus a

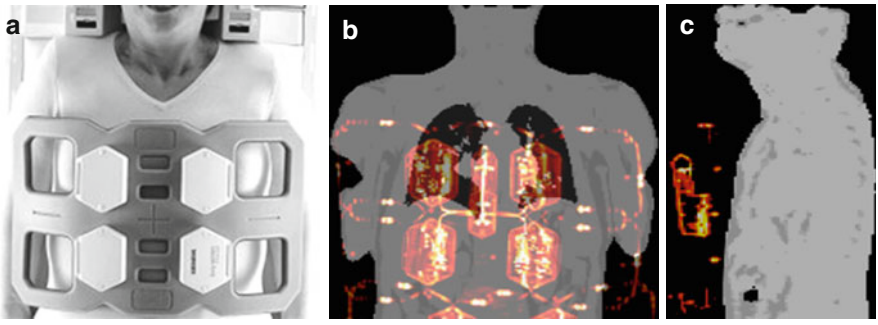


**Fig. 1.6** (**a**) Six-channel thorax radiofrequency coil for MR signal reception during simultaneous cardiac PET/MR data acquisition. Images (**b**, **c**) show MR-based attenuation maps of the patient tissues that were acquired with a 3D Dixon-based sequence. The hardware attenuation correction map of the flexible RF coil (*orange/red color*) here was co-registered with nonrigid registration on the patient tissue attenuation correction map. Such attenuation maps represent the geometric distribution of PET signal-attenuating hardware and soft tissue structures in the PET field of view

pre-acquired rigid 3D CT template cannot directly be co-registered [17]. As alternative strategy for AC of flexible RF coils, visible markers have been proposed to perform an automatic nonrigid co-registration of the pre-acquired 3D CT attenuation template to the individual position and shape of the flexible RF coil during the cardiac PET/MR examination (Fig. 1.6) [17, 19].

## 1.4 Motion Correction (MC)

Integrated PET/MRI systems provide the inherent advantage of simultaneous PET and MR data acquisition. In view of motion correction (MC), this is an inherent advantage over PET/CT that is currently being further explored [20–27]. While in PET/CT the CT data is static and for dose considerations is acquired only once at the beginning at a typical hybrid examination, the MR data in PET/MRI is acquired simultaneously to PET data acquisition, and this applies to data acquisition in each bed position. This inherently leads to less deviation and less gross motion between both imaging modalities when compared to PET/CT imaging. Furthermore, real-time MRI data and 4D MR data of breathing motion can be used to retrospectively motion correct PET data to provide improved fusion of PET and MR data sets [20–27]. This may potentially lead to improved lesion visibility in the lungs, upper abdomen, and liver and may also result in better quantification of activity in the myocardium since all structures are depicted with sharper contours and less smeared over a larger volume which otherwise leads to reduced standardized uptake values (SUV) of regions subject to motion [25].

With the heart being subject to cardiac and breathing motion during PET and MR data acquisition, it is expected that the further development and application of advanced triggering, nonrigid motion correction, and attenuation correction methods will have a substantial impact on PET/MR cardiac imaging in general and more specific in myocardial tissue quantification [26].

### 1.4.1 Cardiac Gating

Most MRI sequences as well as reconstruction of cardiac PET data recorded in list mode require a sufficiently good ECG signal in order to control or selectively use data from an acquired image of a specific cardiac phase. In contrast to PET examinations in PET/CT procedures, during integrated PET/MRI, it must be considered that ECG signals can be significantly influenced by the magnetic field and radiofrequency pulses, thus requiring special care when applying the electrodes and monitoring the ECG signal. The relatively long duration of the simultaneous MRI examination can be used almost in its entirety for the parallel acquisition of PET data; this compensates for the loss of PET acquisition time caused by ECG gating and results in high PET image quality (Fig. 1.7) [4, 27, 28].

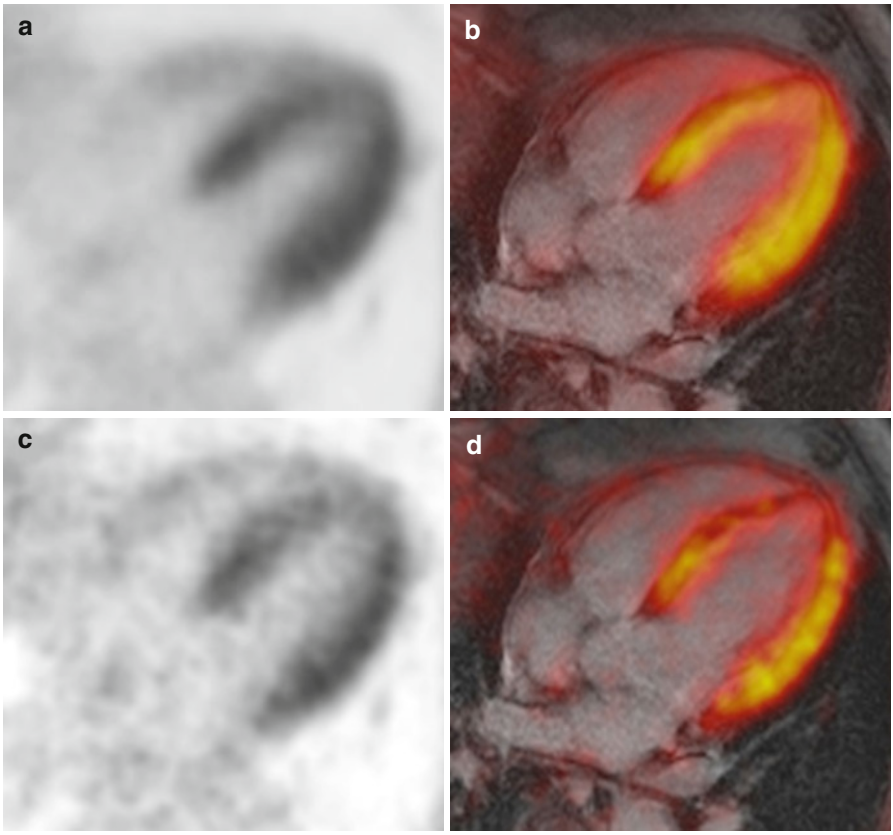


**Fig. 1.7** Impact of ECG gating on cardiac PET imaging. The images show an end-diastolic four-chamber view of PET (**a**, **c**) and PET/MR fused with late gadolinium-enhanced ECG-gated MRI (**b**, **d**). The PET data in (**a**, **b**) was non-ECG gated; the PET data in (**c**, **d**) was ECG gated. While the non-ECG gated PET data (**a**, **b**) here shows better signal-to-noise ratio due to longer data acquisition, the ECG-gated PET data showing one out of eight cardiac motion phases (**c**, **d**) provides sharper depiction of the activity distribution constrained to the myocardial wall

## 1.5 Hybrid Imaging Workflow

Simultaneous and independent PET and MR data acquisition provides the basis for cardiac PET/MRI studies. In view of data synchronization, this acquisition scheme also provides an inherent advantage of cardiac PET/MR when compared to PET/CT since the acquisition times of both imaging modalities are closely matched in PET/MR, while in PET/CT the CT data acquisition is to be finished within few seconds. Thus, the rather long acquisition times of a cardiac MR exam encompassing evaluation of anatomy, function, and perfusion can be used synergistically to extend the acquisition time of PET. This, in combination with PET data acquisition in list

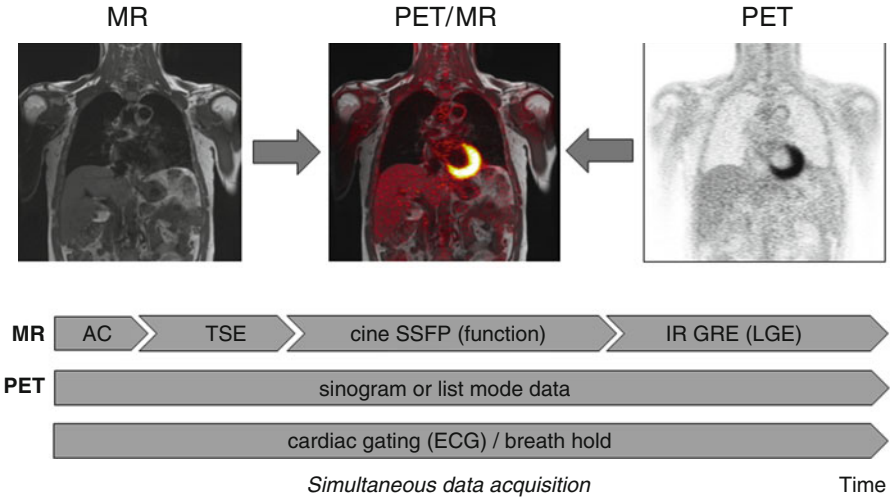


**Fig. 1.8** PET/MR simultaneous imaging workflow. MR (*left*) and PET (*right*) data acquisition is performed simultaneously. The standard cardiac MR examination encompasses sequences for attenuation correction, e.g., turbo spin echo (*TSE*) for anatomic reference and cardiac-gated cine-cine steady-state free precession (*SSFP*) sequences for assessment of cardiac function. Late gadolinium enhancement (*LGE*) using an inversion recovery (*IR*) gradient echo (*GRE*) sequence reveals cardiac infarction that then can be correlated to the metabolic information of simultaneously acquired F18-FDG-PET

**Table 1.1** Challenges and current correction methods relevant for cardiac PET/MRI

| Challenge | Correction method | Reference # |
|---|---|---|
| Attenuation correction of patient tissues | MR-based tissue segmentation into tissue classes (e.g., background air, soft tissues, fat, lung) with Dixon-based MR sequences | [8, 9] |
| Attenuation correction of hardware components | CT-based and energy-converted templates of hardware components (e.g., patient table, RF coils) | [14–19] |
| Motion during MR and/or PET data acquisition | MR-derived motion fields applied to PET reconstruction | [20–27] |
| Motion between MR-based attenuation map and PET data acquisition | Acquisition of multiphase MR-based AC maps during breathing and co-reconstruction of list-mode PET-data to matching AC phase | [24, 25] |

mode, allows for ECG gating or even double gating of cardiac and breathing motion while enough PET data is acquired to support retrospective data reconstruction with good image quality of gated and time-resolved PET studies (Fig. 1.8). All challenges and current correction methods associated with cardiac PET/MRI are listed in Table 1.1.

## 1.6 Summary

Whole-body PET/MR hybrid imaging has entered the clinical arena. On the technical and hardware development level, several challenges had to be overcome that ultimately have led to the availability of integrated whole-body PET/MR systems. Innovative methods have been developed to provide viable solutions for MR-based attenuation correction and motion correction of PET data and are still subject to ongoing research. Unlike any other clinical PET/MR imaging application, cardiac PET/MRI will benefit from further evolution and application of attenuation correction and motion correction algorithms to unveil its full diagnostic potential.

## References

1. Delso G, Furst S, Jakoby B, et al. Performance measurements of the Siemens mMR integrated whole-body PET/MR scanner. J Nucl Med. 2011;52:1914–22.
2. Zaidi H, Ojha N, Morich M, et al. Design and performance evaluation of a whole-body Ingenuity TF PET-MRI system. Phys Med Biol. 2011;56:3091–106.
3. Quick HH. Integrated PET/MR. J Magn Reson Imaging. 2014;39:243–58.
4. Nensa F, Poeppel TD, Beiderwellen K, et al. Hybrid PET/MR imaging of the heart: feasibility and initial results. Radiology. 2013;268:366–73.
5. Rischpler C, Nekolla SG, Dregely I, Schwaiger M. Hybrid PET/MR imaging of the heart: potential, initial experiences, and future prospects. J Nucl Med. 2013;54:402–15.
6. Schlosser T, Nensa F, Mahabadi AA, Poeppel TD. Hybrid MRI/PET of the heart: a new complementary imaging technique for simultaneous acquisition of MRI and PET data. Heart. 2013;99:351–2.
7. Lee WW, Marinelli B, Van der Laan AM, et al. PET/MRI of inflammation in myocardial infarction. J Am Coll Cardiol. 2013;59:153–63.
8. Martinez-Moller A, Souvatzoglou M, Delso G, et al. Tissue classification as a potential approach for attenuation correction in whole-body PET/MRI: evaluation with PET/CT data. J Nucl Med. 2009;50:520–6.
9. Samarin A, Burger C, Wollenweber SD, et al. PET/MR imaging of bone lesions – implications for PET quantification from imperfect attenuation correction. Eur J Nucl Med Mol Imaging. 2012;39:1154–60.
10. Pichler BJ, Judenhofer MS, Catana C, et al. Performance test of an LSO-APD detector in a 7-T MRI scanner for simultaneous PET/MRI. J Nucl Med. 2006;47:639–47.
11. Lecomte R. Novel detector technology for clinical PET. Eur J Nucl Med Mol Imaging. 2009;32:S69–85.
12. Schaart DR, van Dam HT, Seifert S, et al. A novel, SiPM-array-based, monolithic scintillator detector for PET. Phys Med Biol. 2009;54:3501–12.
13. Levin C, Glover G, Deller T, et al. Prototype time-of-flight PET ring integrated with a 3T MRI system for simultaneous whole-body PET/MR imaging [abstract]. J Nucl Med. 2013;54 Suppl 2:148.
14. Carney JPJ, Townsend DW, Rappoport V, Bendriem B. Method for transforming CT images for attenuation correction in PET/CT imaging. Med Phys. 2006;33:976–83.
15. Delso G, Martinez-Möller A, Bundschuh RA, et al. Evaluation of the attenuation properties of MR equipment for its use in a whole-body PET/MR scanner. Phys Med Biol. 2010;55:4361–74.
16. Tellmann L, Quick HH, Bockisch A, Herzog H, Beyer T. The effect of MR surface coils on PET quantification in whole-body PET/MR. Med Phys. 2011;38:2795–805.
17. Paulus DH, Braun H, Aklan, Quick HH. Simultaneous PET/MR imaging: MR-based attenuation correction of local radiofrequency surface coils. Med Phys. 2012;39:4306–15.

18. Paulus DH, Tellmann L, Quick HH. Towards improved hardware component attenuation correction in PET/MR hybrid imaging. Phys Med Biol. 2013;58:8021–40.
19. Kartmann R, Paulus DH, Braun H, et al. Integrated PET/MR imaging: automatic attenuation correction of flexible RF coils. Med Phys. 2013;40(8):082301. doi:10.1118/1.4812685.
20. Tsoumpas C, Mackewn JE, Halsted P. Simultaneous PET-MR acquisition and MR-derived motion fields for correction of non-rigid motion in PET. Ann Nucl Med. 2010;24:745–50.
21. Tsoumpas C, Buerger C, King AP, et al. Fast generation of 4D PET-MR data from real dynamic MR acquisitions. Phys Med Biol. 2011;56:6597–613.
22. Catana C, Benner T, van der Kouwe A, et al. MRI-assisted PET motion correction for neurologic studies in an integrated MR/PET scanner. J Nucl Med. 2011;52:154–61.
23. Brendle CB, Schmidt H, Fleischer S, Braeuning UH, Pfannenberg CA, Schwenzer NF. Simultaneously acquired MR/PET images compared with sequential MR/PET and PET/CT: alignment quality. Radiology. 2013;268:190–9.
24. Wuerslin C, Schmidt H, Martirosian P, et al. Respiratory motion correction in oncologic PET using T1-weighted MR imaging on a simultaneous whole-body PET/MR system. J Nucl Med. 2013;54:464–71.
25. Grimm R, Fürst S, Dregely I, et al. Self-gated radial MRI for respiratory motion compensation on hybrid PET/MR systems. Med Image Comput Comput Assist Interv. 2013;16:17–24.
26. Fieseler M, Kugel H, Gigengack F, et al. A dynamic thorax phantom for the assessment of cardiac and respiratory motion correction in PET/MRI: a preliminary evaluation. Nuc Instr Meth Phys Res A. 2013;702:59–63.
27. Baumgartner CF, Kolbitsch C, Balfour DR, et al. High-resolution dynamic MR imaging of the thorax for respiratory motion correction of PET using groupwise manifold alignment. Med Image Anal. 2014;18:939–52.
28. Nensa F, Schlosser T. Cardiovascular hybrid imaging using PET/MRI. Rofo. 2014;186:1094–101.

# Potential Role of Cardiac PET/MRI in Cardiovascular Disease: Initial Experience

2

Felix Nensa, Thorsten D. Poeppel, and Thomas Schlosser

## 2.1 Introduction

Hybrid PET/MR imaging using sequential and integrated scanner platforms has been available for several years, and from the beginning, expectations toward cardiovascular applications have been high. Both PET and MRI have been used in cardiovascular imaging for decades, and in recent years, MRI became a standard of reference with respect to a variety of cardiovascular diseases. Cardiac MRI allows for the detailed anatomical assessment of the cardiovascular system, quantification of cardiovascular function, and multiparametric tissue classification. PET imaging allows for the precise quantification of myocardial perfusion and coronary blood flow reserve, visualization of specific metabolic processes, as well as quantification on the molecular level. Despite a certain overlap between modalities, the excellent morphologic and functional imaging capabilities of MRI in combination with the high sensitivity and quantification capabilities of PET are poised to provide added value in a variety of cardiac diseases. The following chapter provides a summary of the current state of scientific research in cardiovascular PET/MRI.

F. Nensa, MD (✉) • T. Schlosser, MD
Department of Diagnostic and Interventional Radiology and Neuroradiology, University Hospital of Essen, University of Duisburg-Essen, Essen, Germany
e-mail: felix.nensa@gmail.com; thomas.schlosser@uni-due.de

T.D. Poeppel, MD
Clinic for Nuclear Medicine, University Hospital of Essen, University of Duisburg-Essen, Essen, Germany
e-mail: thorsten.poeppel@uni-due.de



T.H. Schindler et al. (eds.), *Molecular and Multimodality Imaging in Cardiovascular Disease*, DOI 10.1007/978-3-319-19611-4_2

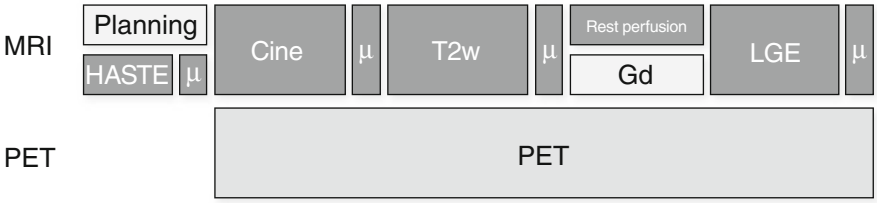


**Fig. 2.1** Basic protocol for simultaneous cardiac PET/MR imaging. *HASTE* axial 2D half Fourier acquisition single-shot turbo spin echo sequence, *μ* attenuation map (μ-map) using 2-point Dixon sequences, *Cine* Cine imaging using balanced SSFP sequence, *T2w* T2-weighted imaging using turbo inversion recovery magnitude sequence, *Rest Perfusion* rest perfusion imaging using saturation recovery fast low-angle shot sequence, *Gd* ~10 min waiting for late gadolinium enhancement, *LGE* late gadolinium enhancement imaging using segmented 2D inversion recovery turbo FLASH sequence

## 2.2 Feasibility

Being clinically well established, cardiac MRI still remains a challenge. Several sources of motion originating from cardiac movement, from breathing, and from multidirectional blood flow require fast and robust imaging, while the involvement of small anatomical structures like papillary muscles or heart valves demands high spatial image resolution. To meet these requirements, cardiac MRI employs highly optimized and complex acquisition techniques, which potentially could be more susceptible to inhomogeneity of the magnetic field. However, despite the presence of PET detectors in the magnetic field of the MR imaging unit, being a potential source of field inhomogeneities, eddy currents, and electromagnetic interference, several reports have demonstrated the technical feasibility and high image quality of cardiac PET/MR imaging on an integrated scanner (Fig. 2.1) [1–5]. Using standard MR sequences for cardiac imaging and dedicated low-attenuation body surface coils, no negative side effects from the integrated imaging system design have been observed [5].

Myocardial PET imaging with FDG usually requires a special dietary preparation [3, 6], which is known to be a source of patient discomfort and potential incompliance. In addition, the relatively long duration of cardiac MRI examinations associated with noise, narrowness, and immobility can result in premature cancellation of examinations by the patient. Indeed, a cardiac PET/MRI study revealed long examination times, the PET/MR imaging examination itself, and fasting to be the main sources of discomfort, resulting in only moderate patient compliance [5]. Thus, it seems mandatory to further optimize patient preparation and implement compact imaging protocols to pave the way for the clinical establishment of cardiac PET/MRI.

## 2.3 MRI-Based Attenuation Correction

Since there is no direct translation of MR-acquired image contrasts into gamma ray attenuation coefficients of tissue, alternative techniques for attenuation correction of PET data had to be developed. While in principle several methods are available [7], currently an MR-based image segmentation approach is typically used in

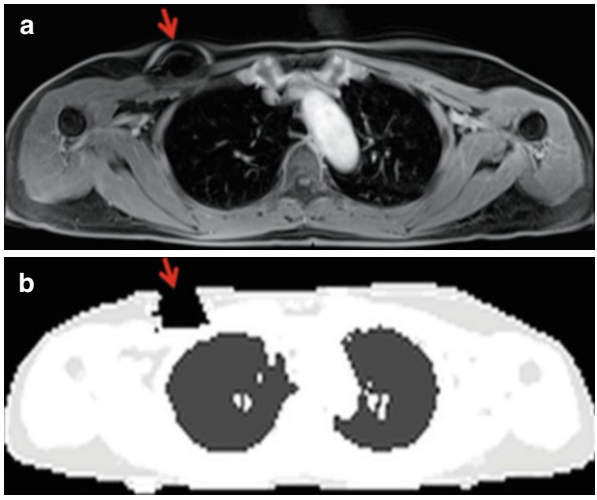


**Fig. 2.2** Source of imaging artifacts. Implanted port system causing MR imaging artifacts (**a**, *arrow*) resulting in erroneous attenuation coefficients in μ-maps (**b**, *arrow*)

integrated cardiac PET/MR imaging [8]. This method usually segments tissue into four compartments (background, lung, fat, and soft tissue) with fixed attenuation coefficients assigned to each compartment. Consequently, the resulting attenuation maps are relatively coarse as finer nuances between tissue attenuations are not represented; e.g., the myocardium vs. the blood, which are both classified as soft tissue. Moreover, the bone is also classified as soft tissue and thus severely misclassified regarding its attenuation for gamma rays. Therefore, in the bone tissue and in its vicinity, standardized uptake values (SUVs) derived from PET/MRI systems might be significantly underestimated when compared to standardized uptake values derived from PET/CT [9]. Using ultrashort echo time (UTE) sequences, the segmentation of tissue with very short T2* (such as the bone) has been demonstrated to be feasible [10]. However, this technique is still limited to a rather small field of view and thus not yet available in cardiac PET/MR imaging.

The segmentation-based approach is dependent on the accuracy of the tissue segmentation algorithm, which can be significantly wrong in the presence of artifacts in the underlying MR images. Artifacts that are frequently found in cardiac imaging often originate from foreign objects like implantable port systems, sternal wire cerclages, artificial heart valves, or artificial joint replacement of the humerus (Fig. 2.2).

Also, cardiac MR imaging is usually performed with the patient's arms aligned along the body axis. In larger patients, this can result in parts of the arms being placed outside the MR field of view, causing so-called truncation artifacts at the edges of the attenuation maps. This can at least partially be avoided by imaging in the arms-up position, extension of the MR field of view [11], or partial correction with PET emission data using maximum-likelihood reconstruction of attenuation and activity (MLAA) [12].

Nevertheless, segmentation-based attenuation correction has been demonstrated to be a reasonably reliable procedure with regard to visual assessment of PET data by the experienced observer [8]. Regarding cardiac PET/MR imaging, it has been shown to provide excellent visual PET image quality that was in good concordance